

## Synthesis and Characterization of Polyvinyl alcohol /Polyaniline/Functionalized Multiwalled Carbon Nanotube Composite by Gamma Radiation Method

Norfazlinayati O.<sup>1</sup>, Talib Z. A.<sup>1\*</sup>, Nik Salleh N.G.<sup>2</sup>,  
Shaari A. H.<sup>1</sup>, and Mohd Hamzah H.<sup>2</sup>

<sup>1</sup>Department of Physics, Faculty of Science, Universiti Putra Malaysia, 43400 UPM Serdang, Selangor

<sup>2</sup>Radiation Processing Technology Division, Malaysian Nuclear Agency, 43000, Bangi, Kajang Selangor

\*Corresponding author: [zainalat@science.upm.edu.my](mailto:zainalat@science.upm.edu.my)

<sup>1</sup>fazlinazah@gmail.com, <sup>2\*</sup>zainalat@upm.edu.my, <sup>3</sup>nik\_ghazali@nm.gov.my,

<sup>4</sup>ahalim@upm.edu.my, <sup>5</sup>hamzah@nm.gov.my

**Abstract.** The composite of functionalized multiwalled carbon nanotube (*f*-MWCNT), polyvinylalcohol (PVA) and polyaniline (PANI) were in-situ synthesized by gamma ( $\gamma$ ) irradiation method. In order to make the free standing composite films, the mixture was cast onto a glass plate and dried before being exposed to irradiation. The formation and incorporation of PANI onto the surface of *f*-MWCNT were confirmed by field emission scanning electron microscopy (FESEM), X-Ray Diffraction (XRD), Fourier Transform Infrared Spectroscopy (FTIR) and UV-Visible (UV-Vis) Spectrophotometer. It was found that in-situ polymerized PANI was coated onto the surface of *f*-MWCNT due to the increase of *f*-MWCNT diameter after irradiation and it is supported by the XRD spectra in which it shows that the intensity of main peak in PANI decreases upon irradiation. The increasing of absorption spectra intensity in the FTIR spectra indicates the polymerization of PANI is occurred. In addition, it was found that quinoid unit in composite film is richer as compared to unirradiated sample. This is supported by UV-Vis analysis that shows the benzenoid ring is excited in which the  $\pi$ - $\pi^*$  transition peak is shifted to the high wavenumber after irradiation. The calculated value for optical energy band gap decreases after irradiated at 50kGy by  $\gamma$ -rays suggested that the resultant composite is more conductive as compared to unirradiated samples.

**Keywords:** conducting polymer, carbon nanotubes, gamma-radiation

### Introduction

Polyaniline (PANI) is a conjugated polymer (CP) that can act as a semiconductor due to the  $\pi$ -electron delocalisation along their polymer backbone. It has been more extensively studied as compared to other conducting polymers due to its tunable electrical conductivity, easy preparation from common chemicals, and excellent thermal and environmental stabilities [1-4]. The uniqueness of PANI is that its conductivity can be controlled by simply doping with acid or dedoping with the use of base materials. When it is doped with acid, PANI will be a conductive polymer in the form of emeraldine salt and with a dark green colour. When it is dedoped with acid, it will turn into a bluish colour, indicating that it is in PANI emeraldine base form. It can also change properties and colours, such as white or colourless for leucoemeraldine form and violet-coloured for (per)nigraniline form, by simply changing the oxidation state during the polymerisation process. The different colours of polyaniline corresponding to the different oxidation states and the acid/base doping response

has led to polyaniline being considered as favourable candidate for acid/base chemical vapour sensors, supercapacitors and biosensors. However, the conjugated polymer does have weak properties such as being insoluble in typical organic solvents due to its strong inter- and intra-molecular interactions and the formation of a crosslinked structure. The low electrical conductivity of polyaniline has also hindered its potential as a replacement for metals. An effective approach to increase the conductivity of a polymer is to introduce conductive filler to the polymer matrix.

Multiwalled carbon nanotubes (MWCNTs) have been widely used especially in the field of nanoscience and nanotechnology. Due to its ideal core materials characteristic by acting as carbonaceous nanofillers, MWCNTs play a crucial role as it possesses structural features and ultra-high charge carrier mobility, huge thermal conductivity, outstanding mechanical strength and high flexibility properties [2]. Therefore, the combination of polyaniline and MWCNT will produce a composite with enhanced properties (e.g. thermal, physical, electronic) than the original material. The combination of PANI and other types of conducting polymers with MWCNTs has been widely applied in various electronic industrial applications including photovoltaic cells, organic light emitting diodes, electromagnetic shielding, electrostatic dissipation, antennas, batteries, supercapacitors, gas sensors, solar cells, optical pH sensing, etc. [5-8].

The first reported work in synthesis of polymer composite and MWCNTs with excellent mechanical property was by Ajayan and coworkers [9] by mixing the MWCNTs with polymer epoxy. Since then, there have been extensive efforts to combine CP and MWCNTs by various methods especially in synthesizing MWCNTs/PANI composites. Among them include solution mixing [10-11], interfacial polymerization [1] in-situ polymerization [12-13] and electrophoretic method [14-15]. However these methods have their own weaknesses. For instance, solution mixing and electrophoretic method are quite expensive due to the reliance in electricity and continuous mixing whereas for in-situ polymerization and interfacial polymerization, these methods are unclean, difficulty to dispose the chemical residues and unscalable.

Gamma irradiation has been used for many years in modification of materials [16]. The major advantages of radiation processing are neither oxidizing agent is used to polymerize PANI nor surfactant agent is needed to functionalize MWCNTs with PANI. Therefore,  $\gamma$ -radiation method promises us to be an eco-friendly technique.  $\gamma$ -radiation is electromagnetic radiation of high frequency and high energy able to liberate an electron from an atom or molecule by altering the chemical bonds and removing electrons from the atoms. In polymer materials, the backbone of the polymer absorbs energy which then liberates free radicals [16]. Moreover, the process of utilising radiation technology is almost free from contaminants. The creation of free radicals is not dependent on the temperature or heat but entirely rely on the absorption of high penetration of radiation energy by polymeric materials. As there is no catalyst involved via the radiation technique, the purity of products is maintained, and consequently the process is clean and cost effective. Earlier work have also shown that  $\gamma$ -radiation can be used to enhance conductivity *cum* oxidation agent in polymerization of PANI [17-18].

In this paper, the preparation and characteristics of free-standing film of PANI/functionalized-MWCNTs (PANI/*f*-MWCNTs) nanocomposites in the PVA matrix using in-situ polymerisation initiated by  $\gamma$ -irradiation method is discussed. The motivation to

embark on this research is to increase the fundamental knowledge on the studied system which will be useful for researchers working towards making this material for technologically important applications.

## Experimental

### *Materials*

The chemicals used in this study were Polyvinyl alcohol, PVA (Merck), aniline hydrochloride, AniHCl (Aldrich) and functionalized multiwalled carbon nanotubes with carboxylic acid, *f*-MWCNTs (Nanostructure & Amorphous Material Inc.). The *f*-MWCNTs have an average diameter of 10-20 nm and length of 20-30  $\mu\text{m}$ . All the materials were used without further purification.

### *Synthesis of PVA/PANI/*f*-MWCNTs composite film*

The PVA/PANI/*f*-MWCNTs composite film was prepared by dissolving 75 pph (0.9 g) of AniHCl monomer in 40 ml of PVA stock. The mixture was then stirred by using a conventional magnetic stirrer for 2 h. Next, 6 pph (0.072 g) of *f*-MWCNTs powder was added to the mixture and ultrasonicated for 2 h by using the water bath technique. The solution was then cast onto a glass plate and dried in an oven at 48-50  $^{\circ}\text{C}$  for 24 to 48 h before being exposed to irradiation. PVA/PANI composite without *f*-MWCNTs as a control samples were also prepared in the same condition

### *$\gamma$ -Irradiation technique*

Irradiation by  $\gamma$ -rays was conducted at room temperature from a Co-60 source at a constant dose rate of 50 kGy. The radiation was accomplished by placing the films in plastic bags and sealed. The sealed bags were placed on aluminium totes which automatically entered and left the radiation room on a roller conveyor system. Totes were conveyed on two levels, lower and upper levels, around a Co-60 source using a two-pass system. This provided the maximum utilisation of ionising energy ensuring that samples were well exposed on all sides. The irradiation duration time took about 25 h to reach the dose at 50 kGy.

### *Characterization*

Field Emission Scanning Electron Microscopy (FESEM) was used to study the surface morphology and dispersion state of the composite films. The films were coated with an extremely thin layer (1.5 - 3.0 nm) of gold, and the analysis was carried out using Nova NanoSEM 230 with an accelerating voltage of 5 kV under 150,000x magnification. The cross section of the composite film was obtained by viewing perpendicular to the film surface using a special designed stub dedicated for cross section SEM measurement. X-ray Diffraction (XRD) analysis was conducted using a computer-controlled x-ray diffractometer (PANalytical X'pert PRO XRD System) with  $\text{CuK}\alpha$  radiation source ( $\lambda=1.540598 \text{ \AA}$ ) generated at an accelerating potential of 40 kV and with a tube current of 30 mA. Fourier Transform Infrared (FTIR) spectra were recorded on Perkin Elmer 1650 spectrometer in the frequency range of 500-4000  $\text{cm}^{-1}$  at room temperature by the ATR method. The optical band

gaps of the composite films were determined from optical absorption spectra obtained from measurement using Shimadzu UV-1800 in the wavelength range of 200 to 1000 nm.

## Results and discussions

### *Morphology*

Figure 1 (a)-(f) present the FESEM images of PVA/PANI and PVA/PANI/*f*-MWCNTs composite films before and after radiation. Figure 1 (a) shows the composite of PVA/PANI for unirradiated film which demonstrated that the nonhomogeneous structure comes from protonated form of AniHCl that were blended together in the PVA matrix. The morphology of the structure changes after irradiation. It can be seen that the  $\gamma$ -radiation leads to the deposition of small clusters of oblong-shaped structures (Figure 1 (b)). The uniform distribution of the elongated structures in the PVA matrix is confirmed by the uniformly green colour of the composite film (Figure 1 (f)). According to the reported research by MacDiarmid and his team [4], the colour changes and the oblong shapes appear when the polymer becomes in the form of emeraldine salts (ES). This can be considered as the first evidence that PANI was successfully polymerised in ES form after being irradiated by in-situ polymerisation process via  $\gamma$ -rays.

After loading *f*-MWCNTs in the composites, agglomerates and clusters of *f*-MWCNTs can be clearly depicted all over the surface of the film (Figure 1 (c)). The agglomeration of *f*-MWCNTs can be seen by the naked eye as shown in Figure 1 (f) (in the circle). After irradiation, the film exhibits better dispersion and has a homogenous structure. This is supported with the uniform dark green colour in the composites film, as shown in Figure 1 (f). Figure 1(e) presents the cross-section of the film where it can be clearly seen that the *f*-MWCNTs are coated with PANI in the PVA web. Therefore, the diameter of the tube has been measured to get an overview of the size difference in which the diameter of the nanotube was taken directly from the operating system (Nova NanoSEM 230). The diameter of the nanotube increased to 80-150 nm after being irradiated as compared to the unirradiated film, which is about 45-62 nm. It is believed that difference in nanotube size before and after irradiation will give indication that PANI has been successfully coated on the outer layer of *f*-MWCNTs [19]

The coating of PANI on *f*-MWCNTs cause the film has homogenous structure. It can be deduced that the carboxylic groups from *f*-MWCNTs create a local defect on the nanotube surface and consequently, some gaps may exist between individual *f*-MWCNTs to allow the aniline molecules to move into the gaps [20]. It then follows through in-situ polymerization of PANI and *f*-MWCNTs initiated by  $\gamma$ -radiation. The expansions of the PANI polymer chain on the *f*-MWCNTs outer layer would wedges away the bundles of *f*-MWCNTs and break the agglomerations. Thus, PANI/*f*-MWCNTs composites are uniformly dispersed very well in the PVA matrix.



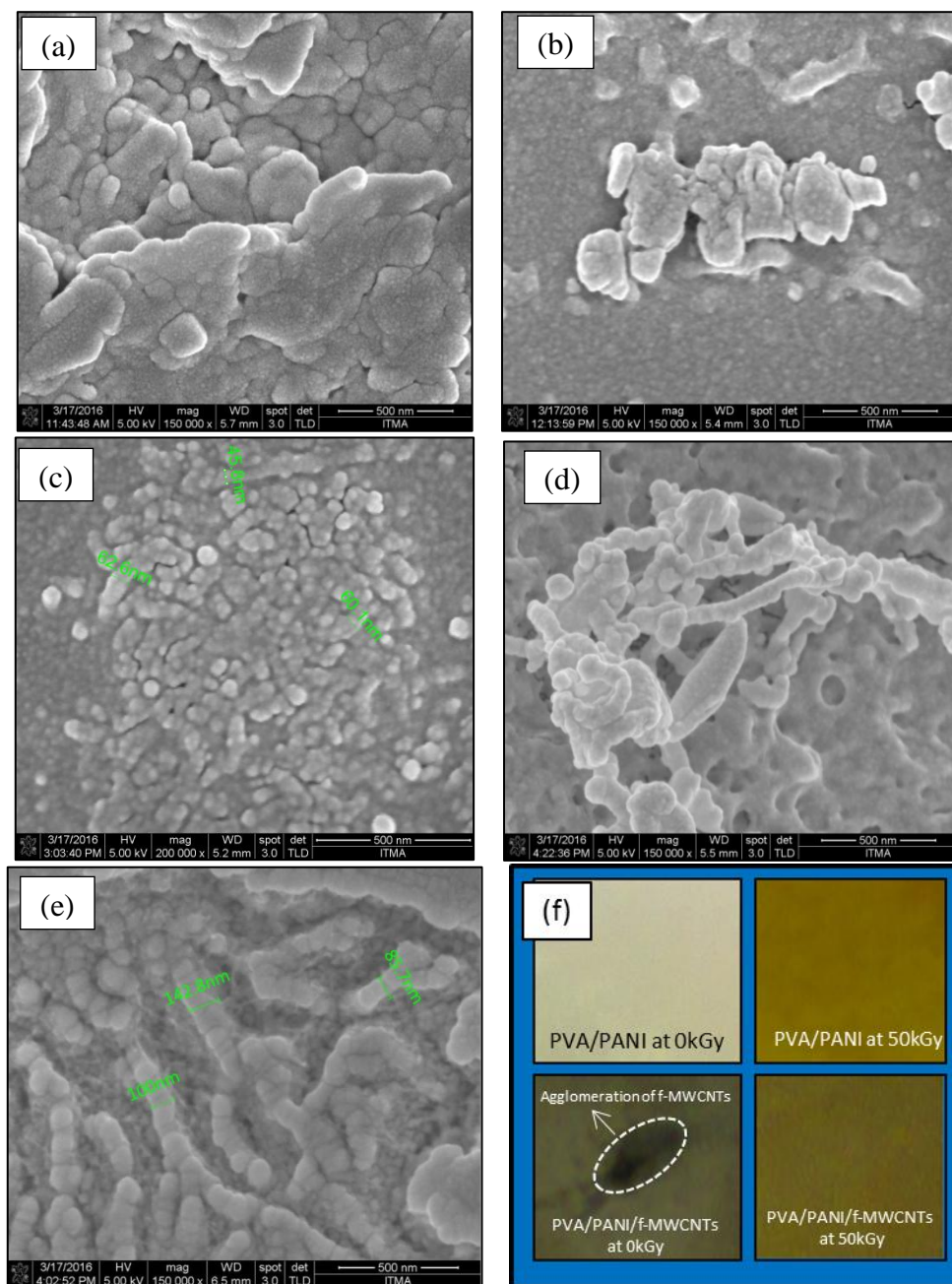


Fig. 1: FESEM micrograph of (a) PVA/PANI before  $\gamma$ -irradiation, (b) PVA/PANI after  $\gamma$ -irradiation at 50 kGy, (c) PVA/PANI/f-MWCNTs before  $\gamma$ -irradiation, (d) PVA/PANI/f-MWCNTs after  $\gamma$ -irradiation at 50 kGy, (e) cross section of PVA/PANI/f-MWCNTs after  $\gamma$ -irradiation at 50 kGy, and (f) film response towards  $\gamma$ -irradiation

### *X-ray Diffraction*

The XRD patterns of the as-synthesized films are shown in Figure 2. It was seen that the first reflection peak near  $2\theta$  at  $19^\circ$  shows the characteristic of crystalline and amorphous phases of conventional semi-crystalline PVA in the PVA/PANI composite film. After the film was irradiated by  $\gamma$ -rays the PVA peak does not show any shift in peak position or changes in intensity. This can be assumed that there is no interruption in the PVA chains before and after the irradiation, which proves that PVA successfully acts as a binder in the

composite film [21-22]. However, the peak did slightly shift about  $1^{\circ}$  to the high angle side after *f*-MWCNTs loaded in the composite film. The intensity of the peak also decreased and became broader after irradiation. This signifies that the polymer planes was slightly disrupted and distorted due to some interruption from *f*-MWCNTs toward the PVA chain. It is believed that due to the presence of carboxylic group (COOH<sup>-</sup>) from *f*-MWCNTs obstructs the crystallisation of the PVA polymer [23].

The crystalline peaks near  $2\theta$  of  $21^{\circ}$  and two other peaks at  $21.9^{\circ}$  and  $22.8^{\circ}$  in the XRD spectra of unirradiated PVA/PANI composite film are attributed to the polymer chain of PANI. After the PVA/PANI composite films have been irradiated at 50kGy, more peaks began to appear between  $2\theta$  of  $23^{\circ}$  to  $36^{\circ}$  (i.e 23.9, 24.9, 25.7, 26.7, 27.6, 28.5, 29.9, 33.4, 34.7 and  $35.6^{\circ}$ ). These peaks may arise due to the regular repetition of aniline monomer in polymer chain [24-25]. Upon irradiation, chlorine anion dissociates from AniHCl group producing Cl free radical thus the defect occurred. The radiation created Cl anion produced from hydrochloride group is captured by neighboring aniline monomers thus forming conducting emeraldine salt of PANI [26]. All of these peaks are sharper and the peak intensity is also increased in comparison with the unirradiated film. Thus, it shows that the irradiated film at 50 kGy has more crystallinity than the unirradiated film.

However, after the *f*-MWCNTs loaded in the composite film, it is observed that the *f*-MWCNTs peak ( $2\theta$  at  $25^{\circ}$  and  $43^{\circ}$  [27]) are absent in the diffractogram of PVA/PANI/*f*-MWCNTs composite film. It is believed that the peak of *f*-MWCNTs is merged peak of PANI. This suggests that during the stirring process the amine groups ( $-\text{NH}_3^+$ ) from the aniline monomer are attached to the surface of the nanotubes which has defect sites on the surface with terminal carboxylic acid group ( $-\text{COOH}-$ ), allowing covalent linkages of the oligomer chain or vice versa [28-30]. This modification is known as the “grafting to” approach [31]. After PVA/PANI/*f*-MWCNTs composite film irradiated at 50 kGy the *f*-MWCNTs peaks are still absent. The characteristic intensity of the dominant PANI peak ( $2\theta$  at  $21^{\circ}$ ) decreases after the irradiation as compared to the film before the irradiation which it is believed that the PANI conducting polymer was coated over the *f*-MWCNTs [25].

Several studies have reported the various possible interactions between PANI and *f*-MWCNTs in the composites. One of the first suggestions is the occurrence of two conditions at a time. The first condition is the PANI becomes a conducting polymer by in-situ polymerisation initiated by  $\gamma$ -rays and the second condition is PANI become interconnected with *f*-MWCNTs during the irradiation process. For the first condition,  $\gamma$ -irradiation has generated reactive sites on the AniHCl monomer leading to the propagation of reaction by Compton scattering or photoelectric effect. The reaction that can be explain is the energy from the  $\gamma$ -rays can make a defect on the very weak bond of the aniline monomers ring ( $-\text{NH}_3^+$ ) to get doped with  $\text{Cl}^-$  and become a dimer of PANI. This is known as an in-situ polymerisation process [32]. It will continuously occur in a very fast way during the polymerisation process until it become complete as a polymer backbone [33]. At the same time also applies to the second condition. The second condition is the carboxylic groups ( $-\text{COOH}$ ) of *f*-MWCNTs are most likely the sites of interaction with hydrogen bonding between the amino groups of aniline monomer ( $-\text{NH}^+$ ) which cause the aniline monomers to adsorb or embed onto the surface of the nanotube.

Consequently, the combinations of the two processes continuously occur during polymerisation by  $\gamma$ -rays which result in PANI coating over the *f*-MWCNTs. Thus, the diffraction peaks of *f*-MWCNTs overlap with multi-coats of PANI and make the crystallinity become low as compared to the unirradiated PVA/PANI composite. Scheme 1 presents a schematically possible formation mechanism of the polymerisation of PANI/*f*-MWCNTs that occurs in the composites.

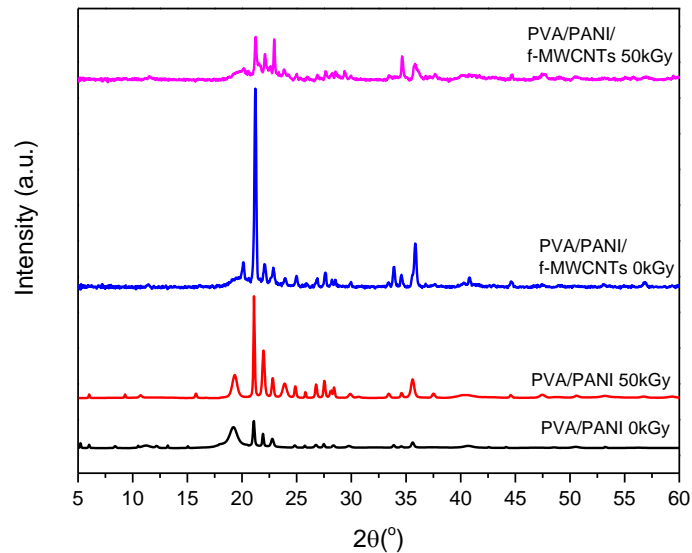
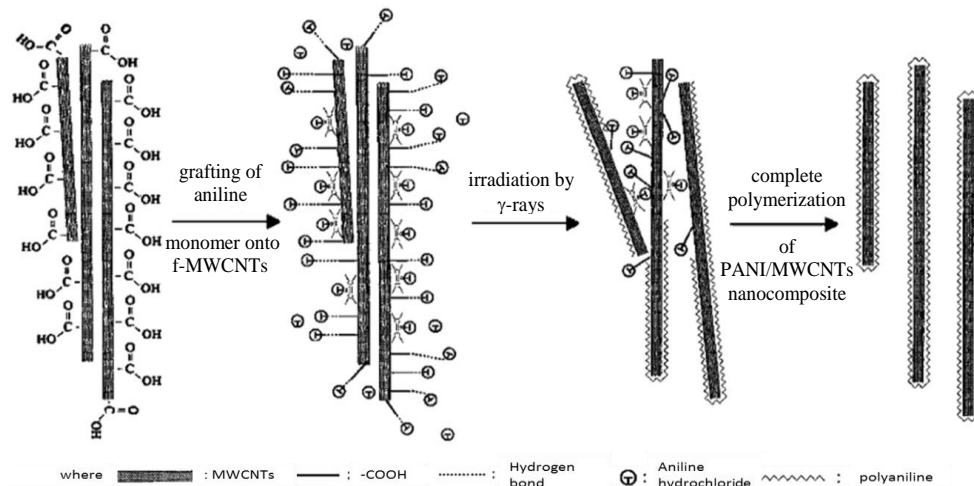


Fig. 2: XRD spectra of PVA, PVA/PANI, and PVA/PANI/*f*-MWCNTs composite films before and after  $\gamma$ -irradiation at 50 kGy



Scheme 1: Possible reaction mechanism of PANI/*f*-MWCNTs composite during in-situ polymerisation by  $\gamma$ -radiation [17-18]

FTIR

Figure 3 displays the FTIR spectra in order to provide information on the chemical structures of PVA/PANI and PVA/PANI/*f*-MWCNTs before and after  $\gamma$ -irradiation. The peaks appear in region 'A', between  $3500\text{--}2250\text{ cm}^{-1}$ , is ascribed to the stretching vibration of O-H and N-H bonds of PVA and PANI [34]. The stretching of the O-H bond from the PVA matrix can be observed at  $3315\text{ cm}^{-1}$  which the broad peak represents the superposition of multiple polymeric H bonds associated with the crystalline and amorphous phases of conventional semi-crystalline PVA [35]. The intensity of the peak decreases after irradiation and diminishes after *f*-MWCNTs loading in the composite film. The peak at  $914\text{ cm}^{-1}$  represents the syndiotactic structure of PVA which corresponds to C-H rocking vibration and also show a decrease intensity after irradiation and *f*-MWCNTs loading [36]. This result suggests that the hydrogen bonding becomes weaker due to the reduction in the number of OH groups, and the polymeric structure is disturbed due to the interruption from PANI and *f*-MWCNTs during irradiation. The disruption of the plane structure is further supported by the decreasing intensity after the irradiation which near absorption bands at  $2903$ ,  $1429$ ,  $1324$ , and  $1093\text{ cm}^{-1}$ , corresponding to C-H stretching, C-H bending, C-H wagging, and C-O stretching vibration, respectively.

The FTIR spectra of PANI show that characteristic band at  $3039\text{ cm}^{-1}$  corresponds to the secondary amines from aromatic C-H stretching vibration and have a combination and overtone band appear in the  $2007\text{ cm}^{-1}$  region [34]. The absorption bands at  $2810\text{ cm}^{-1}$  and  $2584\text{ cm}^{-1}$  corresponding to the N-H stretching vibration arise from the asymmetrical and symmetrical  $\text{NH}_3^+$  groups from salts of amines, respectively [34]. Also, the bands at  $1589\text{ cm}^{-1}$  and  $1479\text{ cm}^{-1}$  are ascribed to the C=C stretching vibration of quinoid (Q) and benzenoid (B) rings [3,37]. The average calculated value of intensity  $I_Q/I_B$  ratio was about 1.12, which suggests that the composite film is mostly composed of quinoid groups. It was further noted that after irradiated at 50 kGy, the intensity of the two bands increases and narrower with  $I_Q/I_B$  ratio increase to 1.16. This suggests that quinoid units are richer than that of the unirradiated film. The increasing intensity also observed for all peaks in composite films reveal that the chain of PANI has longer conjugation lengths as compared to the PVA/PANI unirradiated film [38].

After the addition of *f*-MWCNTs in the composite film and after irradiated by  $\gamma$ -rays, the intensity peaks for the Q and B rings decreased as compared to the PVA/PANI film. The  $I_Q/I_B$  ratio was about 1.09 and further decreased to 1.05 after irradiation. The decreasing ratio may be due to the increase of PANI chain structures causing the Q units to become scattered along polymer chains in the composite film [39]. This signifies that the  $\pi$ -bonded surface of *f*-MWCNTs strongly interacts with the conjugated structure of PANI which confirms that the PANI layer is coated on the *f*-MWCNTs sidewalls [38,40]. However, the peak typically seen with *f*-MWCNTs is found to be absent, indicating that the reaction with (-COOH-) and the formation of amides were complete [8]. Table 1 presents the vibrational assignments for PVA/PANI and PVA/PANI/*f*-MWCNTs composite films.



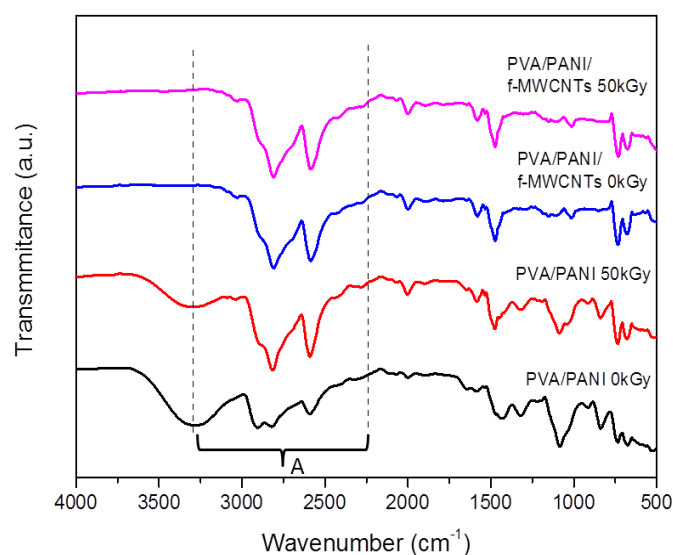


Fig. 3: FTIR spectra of PVA/PANI and PVA/PANI/f-MWCNTs composite films

Table 1: FTIR peak assignments for PVA/PANI at 0 kGy, PVA/PANI at 50 kGy, PVA/PANI/f-MWCNTs at 0 kGy, and PVA/PANI/f-MWCNTs at 50 kGy

Assignment	Wavenumber (cm <sup>-1</sup> )
O-H stretching	3315
C-H stretching of aromatic unit	3039
C-H stretching	2903
N-H stretching from asymmetrical amines group	2810
N-H stretching from symmetrical amines group	2584
C-H stretching of aromatic unit	2007
C=C stretching of quinoid ring	1589
C=C stretching of benzenoid ring	1479
C-H bending	1429
C-H wagging	1324
C-O stretching	1093
C-H rocking	914
C-C stretching	835
N-H out-of-plan bending	738
C-H out-of-plan bending	678

### UV-Vis

Optical absorption spectra of the composite films are displayed in Figure 4. The UV visible spectrum of unirradiated PVA/PANI film shows a sharp intense band at 348 nm which correspond to  $\pi-\pi^*$  transition within the benzenoid rings and a very broad band at 845 nm which correspond to  $\pi-\pi^*$  transition within the quinoid rings as shown in Figure 4 (a) [8,41-42]. After 50 kGy of  $\gamma$ -radiation, the peak at 348 nm shows a hyperchromic effect arising from extended conjugation of polymer length [43]. The growing of PANI chains is confirmed with the band shifting from 845 to 817 nm and broadening of the peak which indicates the absence of delocalized electronic structure that can be signified as the increases in oxidation level of PANI [8, 42]. It was further observed that a new and weak peak near 275 nm arises

after the irradiation which is attributed to  $n-\pi^*$  transition and  $\pi-\pi^*$  transition. The peak represents the chromophoric aspect of PANI that is responsible for the film's color change to green [4,44-45]. The peak can be clearly observed after  $f$ -MWCNTs loading in the composite (Figure 4 (b)).

For the unirradiated PVA/PANI/ $f$ -MWCNTs composite films, three main absorption bands at 270 nm, 337 nm, and 817 nm (Figure 4 (b)) were observed. After the irradiation, the bands at 337 nm present a noticeable shift to 354 nm. The shift is due to the benzenoid ring's excitation and the  $\pi-\pi^*$  transition may involve a strong interaction between aniline monomer and functionalized MWCNTs [7]. The growing of PANI chains is confirmed with the band shifting from 817nm to 824nm. The shifting band presents more of conducting ES form of the polymer which is assigned richer of quinoid rings as compared to the unirradiated film [19]. However, there is no absorption for  $f$ -MWCNTs was observed and this result was consistent with reported work from other researchers [7,19,33].

Optical energy band gap can be determined using equation  $\alpha(\nu)hv=A(h\nu-E_g)^n$  where  $E_g$  is the energy band gap,  $\alpha$  is the absorption coefficient,  $\nu$  is the frequency, and  $A$  constant and  $n$  could be 0.5, 1.5, 2, or 3 depending on the mode of transition. The band gap is extracted from the extrapolation the straight line portion of the plot  $(\alpha(\nu)hv)^2$  versus  $h\nu$  (Figure 5) with axis at  $\alpha=0$ . For this experiment,  $n=0.5$  offered the best fit for all composite films which present the allowed indirect band gap. The measured  $E_g$  value is 2.7, 3.1, 2.8, and 2.8 eV for PVA/PANI 0kGy, PVA/PANI 50kGy, PVA/PANI/ $f$ -MWCNTs 0kGy, and PVA/PANI/ $f$ -MWCNTs 50kGy, respectively. The range for calculated value of  $E_g$  indicates that all the CP synthesised in this study can be classified as organic semiconductors and is due to  $\pi-\pi^*$  transition from valance band to conduction band.

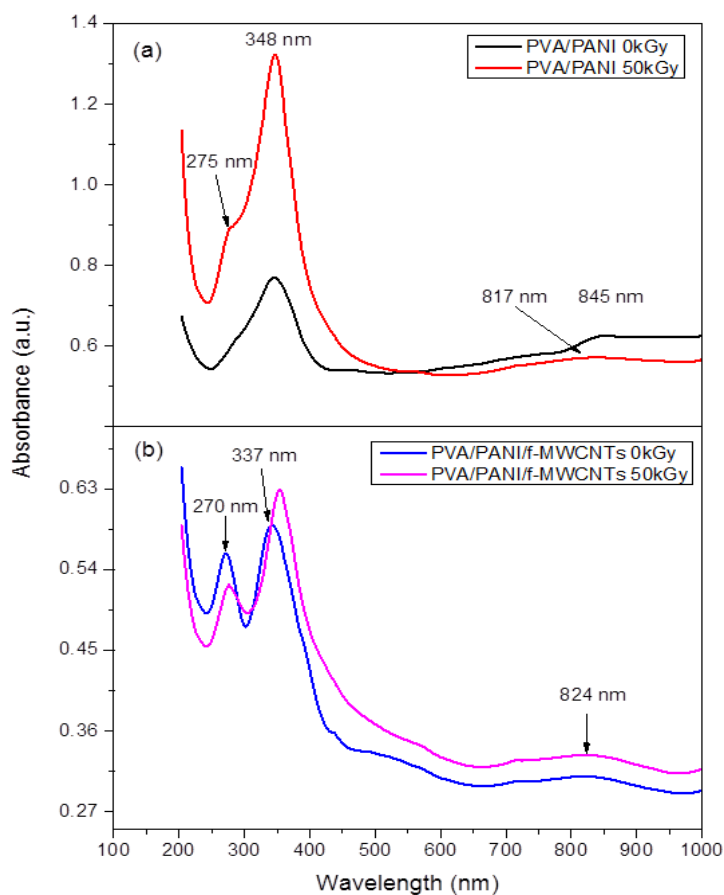


Fig. 4: UV-Vis absorption spectra of PVA/PANI and PVA/PANI/f-MWCNTs composite film

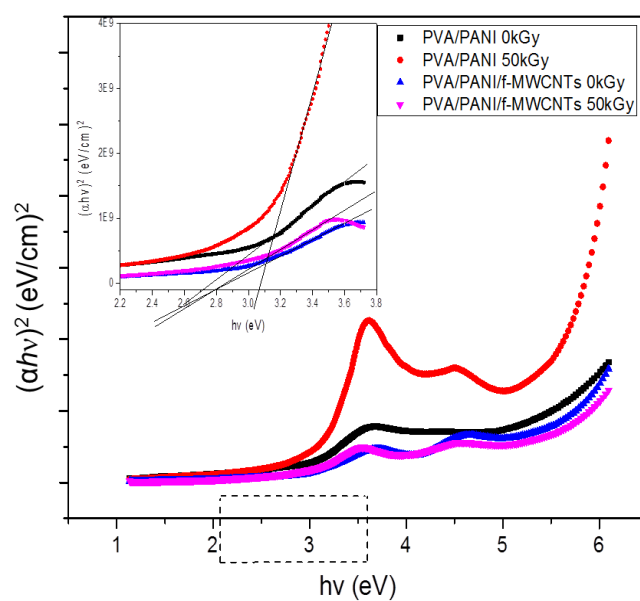


Fig. 5: Band gap of PVA/PANI and PVA/PANI/f-MWCNTs composite film

In addition, closer observation shows that the  $E_g$  for PVA / PANI irradiated film increased as compared to the unirradiated film. This indicates that there is benzenoid-quinoid

bond alteration as known as defect of the conjugated main chain from planar structure occurs during the in-situ polymerisation by  $\gamma$ -radiation process [45]. After the *f*-MWCNTs loaded in the composites, the  $E_g$  decreases to 2.8 eV indicates that more existence of quinoid unit structure in the conjugated polymer main chain [46]. The existence of more quinoid shows the strong intermolecular interaction in the planar main chain of PANI and *f*-MWCNTs. While the value  $E_g$  for PVA / PANI / *f*-MWCNTs film does not change compared to before and after irradiation. It is believed that the value is only comes from the energy band of PANI since the nanotube has been fully coated by PANI. It can be assumed that the functionalized systems could exhibit some degree of disorder in the nanocomposite system. Therefore the degree of disorder in the polymer chain can be estimated through the calculation of Urbach energy or the Urbach tail by using equation

$$\alpha(h\nu) = \alpha_o \exp\left(\frac{h\nu}{E_u}\right)$$

where  $\alpha_o$  and  $E_u$  are a constant and Urbach energy, respectively. The  $E_u$  band gap is extracted from the extrapolation the straight line part of the plot  $\ln \alpha$  as a function of  $h\nu$  with axis at  $\alpha = 0$ . The inverse of the value at  $\alpha = 0$  gives  $E_u$ . Figure 6 show plots of  $\ln \alpha$  versus photon energy,  $h\nu$ . The calculated  $E_u$  are 0.34, 0.36, 0.28 and 0.38 eV for PVA/PANI 0kGy, PVA/PANI 50kGy, PVA/PANI/*f*-MWCNTs 0kGy, and PVA/PANI/*f*-MWCNTs 50kGy, respectively. The obtained values of the Urbach energies and band gap energies are compared as shown in Figure 7. Thus shows that the rise of disordered structure in the composite film and nanocomposite after irradiated, respectively. This indicates that localized state formation in the PANI chains is increasing in the composite and nanocomposite [47].

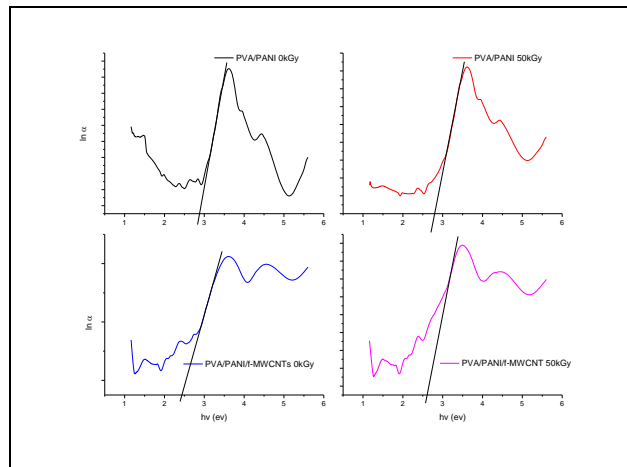


Fig. 6: The Urbach energy ( $E_u$ ) tail for composite and nanocomposite films



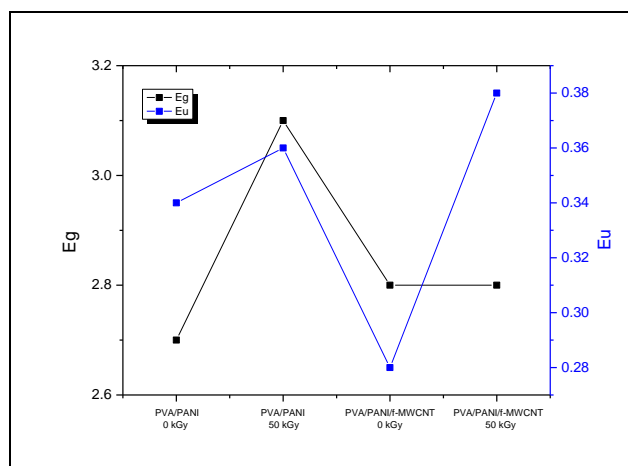


Fig. 7: Variation of the energy band gap  $E_g$  and Urbach energy ( $E_u$ )

## Conclusions

The composite films of PVA/PANI and PVA/PANI/*f*-MWCNTs were successfully synthesized via  $\gamma$ -radiation technique. Surface morphology analysis described that *f*-MWCNTs exhibit a uniform dispersion in the PVA matrix and the diameter of *f*-MWCNTs is significantly increased upon the coating of PANI chains on the outer surface of the nanotube after being irradiated by  $\gamma$ -radiation. The result is supported by XRD data in which the peaks of the composite film are dominated by PANI characteristic peaks. It is believed that the peak for *f*-MWCNTs is merged with the PANI and thus, compromising its appearance. FTIR analysis confirms that PANI was polymerized in emeraldine salt form during the irradiation. FTIR also portrays that the composite film is mostly composed of quinoid groups after the addition of *f*-MWCNTs in the composite film and after irradiated by  $\gamma$ -rays which demonstrate that increased of PANI chains coated over the side wall of the *f*-MWCNTs. The observation is supported by results from UV-Visible analysis which shows shifted band of the  $\pi$ - $\pi^*$  transition indicating that the presents of more quinoid rings. The optical energy band gap exhibited a decreased in value of indicating that the aniline monomer is regularly adsorbed and coated onto the outer layer of *f*-MWCNTs. These results suggests that the conductivity and optical properties were improved after the composite film was irradiated by  $\gamma$ -radiation

## Acknowledgments

This work was supported by UPM Research Grant Scheme. The authors acknowledged the Malaysian Nuclear Agency for their technical assistance.

## References

- [1] Jeon, I., Tan, L., Baek, J., 2010. J. Polym. Sci. Part A: Polym Chem. 48,1962-1972.
- [2] Kumar, AM., Gasem, Z. M., 2016. Polym. Test. 50, 83-93.
- [3] Tang, S. J., Wang, A. T., Chiu, K. C., Lin, S.Y., Huang, K.Y., Yang, C. C., Yeh, J. M., 2011. Polym. J. 43,667-675.
- [4] MacDiarmid, A.G., 2001. Angew. Chem. Int. Ed. 40, 2581-2590.
- [5] Thakur, A.K., Deshmukh, A.B., Choudhary, R.B., Karbhal, I., Majumder, M., Shelke, M. V.,

- (2017) *Mater. Sci. Eng. B* 223,24-34.
- [6] Abdulla, S., Mathew, T. L., Pullithadathil, B., 2015. *Sensor Actuator B*, 221, 1523-1534.
- [7] Bachav, S.G., Patil, D.R., 2015. *Amer. J. Mater. Sci.* 5(4), 90-95.
- [8] Kulkarni, M.V., Kale, B. B., 2013. *Sensor Actuator B*.187, 407-412.
- [9] Ajayan, P. M., Stephan, O., Colliex, C., Trauth, D., 1994. *Compos. Science*, 265, 1212-1214.
- [10] Abd Razak, S. I., Ahmad, A.L., Zein, S.H.S., 2009. *J Phys. Sci.* 20(1), 27-34.
- [11] Ben-Valid, S., Dumortier, H., Decossas, M., Sfez, R., Meneghetti, M., Bianco, A., Yitzchzik, S., 2010. *J. Mater. Chem.* 20, 2408-2417.
- [12] Philip, B., Xie, J., Chandrasekhar, A., Abraham, J., Varadan, V. K., 2004. *Smart Mater. Struct.* 13, 295-298.
- [13] Yang, J., Wang, X., Jia, R., Huang, J., 2010. *J. Phys. Chem. Solid.* 71, 448-452.
- [14] Dhand, C., Arya, S. K., Singh, S. P., Datta, M., Malhotra, B. D., 2008. *Carbon* 46, 1727-1735.
- [15] Fahdil, O., Khalid, S. H., Mokhtar, M., Yusof, A. M., Alias, A. N., Zaine, I. S., 2011. *Key Eng. Mater.* 701, 33-41.
- [16] Charlesby, A., 1965. *Rep. Prog. Phys.* 28, 464-518.
- [17] Bodugoz, H., Guven, O., 2005. *Nucl. Instrumen. Method Phys. Res. B.* 236, 153-159.
- [18] Ali, M. A., Saion, E., Yahya, N., Kassim, A., Dahlan, K. Z., Hashim, S. 2007. *J. Eng. Sci. Technol.* 2(1), 111-118
- [19] Nguyen, V.H., Shim, J. J., 2015. *J. Spectrosc.* 2015, 1-9.
- [20] Rauwel. P., Galeckas, A., Salumaa, M., Ducroquet, F., Rauwel, E., 2016. *Beilstein J. Nanotechnol.* 7, 1075-1085.
- [21] Mahmoud, W. E., Al-Ghamdi, A. A., Kadi, M. W., 2012. *Radiat. Phys. Chem.* 81, 693-696.
- [22] Bhat, N. V., Nate, M. M., Gore, A. V., Bhat, R. M., 2008. *J. App. Polym. Sci.* 110, 2243-2252.
- [23] Bin, Y., Mine, M., Koganemaru, A., Jiang, X., Matsuo, M., 2006. *Polymers* 47, 1308-1317.
- [24] Goswami, M., Mukherjee, A., Das, A. K., Ghosh, R., Meikap, A. K., 2017. *Adv. Nat. Sci.: Nanosci. Nanotechnol.* 8, 1-8.
- [25] Chakraborty, G., Meikap, A. K., Gupta, K., Rana, D., 2012. *Adv Nat Sci: Nanosci Nanotechnol* 3,035015:1-8.
- [26] Mohd Hamzah, H., Saion, E., Yahya, N., Kassim, A., Mahmud, E., Hussain, M. Y., Mustafa, I. S., Ohman, A., Yusof, N. M., Omer, M. A. A., 2007. *J. Nucl. Related Technol. Special Edition* 4, 1-11.
- [27] Yao, X., Kou, X., Qiu, J., 2016. *Organ. Electron.* 38, 55-60.
- [28] Ghatak, S., Chakraborty, G., Meikap, A. K., Woods, T., Babu, R., Blau, W. J., 2011. *J. Appl. Polym. Sci.* 119, 1016-1025.
- [29] Reddy, K. R., Sin, B. C., Ryu, K. S., Kim, J. C., Chung, H., Lee, Y., 2009. *Synth. Met.* 159, 595-603.
- [30] Wu, T. M., Lin, Y. W., 2006. *Polymers* 47, 3576-3582.
- [31] Spitalsky, Z., Tasis, D., Papagelis, K., Galiotis, C., 2010. *Progr. Polym. Sci.* 35, 357-401.
- [32] Sharma. K., Kaith, B. S., Kumar, V., Kalia, S., Vinod, K., Swart, H. C., 2014. *Polym. Degrad. Stab.* 107, 166-177.
- [33] Lee, K. P., Gopalan, A. I., Santhosh, P., Lee, S. H., Nho, Y. C., 2007. *Compos. Sci. Technol.* 67, 811-816.
- [34] Silverstein, R. M., Webster, F. X., Kiemle, D. J., 2005. *Spectrometric identification of organic compounds. Infrared spectroscopy* 7th Edition.
- [35] Shehap, A. M., 2008. *Egypt J. Solid.* 31(1), 75-91
- [36] Mahendia, S., Tomar, A. K., Goyal, P. K., Kumar, S., 2013. *J. Appl. Phys.* 113(073103), 1-7
- [37] Oliveira, L. R., Manzato, L., Mascarenhas, Y. P., Sanches, E. A., 2017. *J. Mol. Struct.* 1128, 707-717
- [38] Nagaraja, M., Mahesh, Manjanna, J., Rajanna, K., Kurian, M. Z., Lokesh, S.V., 2012. *J. Electron. Mater.* 41(7), 1882-1885.
- [39] Sobha, A.P., Narayanankutty, S. K., 2015. *Mater Sci Semicond Process* 39, 764-770
- [40] Liu, W., Wang, S., Wu, Q., Huan, L., Zhang, X., Chen, M., Yao, C., 2016. *Chem. Eng. Sci.* 156, 178-185.

- [41] Gopalakrishnan, K., Elango, M., Thamilselvan, M., 2012. Scholars Research Library Arch. Phys. Res. 3(4), 315-319.
- [42] Adhikari, S., Banerji, P., 2009. Synt. Met. 159, 2519-2524.
- [43] Honmure, S., Ganachari, S. V., Bhat, R., Kumar, H. M. P. N., Huh, D. S., Venkataraman, A., 2012. Int. J. Sci. Res. 1(2), 102-106.
- [44] Shehap, A. M., 2008. Egypt. J. Solid. 31(1), 75-91.
- [45] Mullekom, H. A. M., Vekemans, J. A. J. M., Havinga, E. E., Meijer, E. W., 2001. Mater. Sci. Eng. 32, 1-40.
- [46] Li. Y., 2015. Organic Optoelectronic Materials Book. Chapter 2: Conducting Polymers 23-50.
- [47] Bafandeh N., Larijani M.M., Shafiekhani A., Hantehzadeh M.R., Sheikh N., 2016. Chin. Phys. Lett. [33 \(11\), 117801](#).